Available online at www.sciencedirect.com

ScienceDirect

Ceramics International 40 (2014) 4649–4654

CERAMICS INTERNATIONAL

www.elsevier.com/locate/ceramint

Effect of solids concentration on pore structure of ZnO-foams prepared by particle-stabilized foaming route

Jhen-Jie Jhao, Meng-Hsuan Yang, Wenjea J. Tseng*

Department of Materials Science and Engineering, National Chung Hsing University, 250 Kuo Kuang Road, Taichung 402, Taiwan

Received 20 July 2013; received in revised form 31 August 2013; accepted 2 September 2013
Available online 1 October 2013

Abstract

An initially hydrophilic zinc oxide (ZnO) surface with a contact angle (θ) of $\sim 32^\circ$ has been changed to hydrophobic ($\theta \sim 90^\circ$) through preferential adsorption of anionic sodium dodecul sulfate molecules on the particle surface by electrostatic interactions. Macroporous ZnO foams are prepared by anchoring the hydrophobic ZnO nanoparticles at the air/water interface to stabilize the air-in-water bubbles produced by mechanical frothing, followed then by sintering at elevated temperatures. Solids concentration (ϕ) of the ZnO suspensions is found critically important to pore structure of the sintered ZnO foams; in which, a broad pore-size distribution ($\sim$20–160 μm) results and the pore volume decreases pronouncedly from 2.41 mL g^{-1} to 0.85 mL g^{-1} when ϕ was increased from 3 vol% to 6 vol%. The pore-volume difference stems primarily from the degree of coverage of the nanoparticles on the bubble surface. This is particularly pronounced for the suspension with ϕ of 3 vol%; to which, interconnected spherical pores with a highly porous wall structure are formed because of the insufficient coverage. The process is indeed facile and is readily applicable to "one-pot" preparation of composite foams, such as ZnO foams decorated with discrete distribution of silver particles.

Keywords: D. ZnO; Emulsion; Foam; Porous Material

1. Introduction

Porous zinc oxide (ZnO) ceramics with tailored structure and functionality in powder, film, or bulk form have received increasing attention owing to potential applications in catalysis, sensing, optics, chemical separation, and dye-sensitized solar cell [1–8]. In view of the literature, different synthesis methods have been used to prepare the ZnO ceramics with desired pore architectures. For the synthesis of ZnO particles, Barick et al. [1] prepared pure and doped ZnO nanocrystal bundles by chemical precipitation from zinc acetate precursors in diethylene glycol solvent. The synthesized ZnO nanoclusters with interconnected, three-dimensional pore channels exhibited strong photocatalysis performance under UV irradiations. Li et al. [2] also prepared particulate ZnO aggregates by the chemical precipitation. The porous aggregates were found highly sensitive to poisonous hydrogen sulfide (H_2S) gas. Similarly, Zheng et al. [3] reported chemical preparation of porous, nanostructured ZnO bundles with well-defined shapes by controlling the morphology of zinc oxalate precursors. Muruganandham et al. [4] further observed a decreasing dependence of reaction time required for the formation of macroporous ZnO nanobundles when decomposition temperature of the zinc oxalate precursors was increased. The increased decomposition temperature led to a much more pronounced particle aggregation. For the preparation of porous ZnO films on conductive substrates, electrochemical deposition was often used [6,9–11]. McLachlan et al. [6] and Yeo et al. [9] obtained ZnO films with a uniform pore structure of long-range periodicity via the template-assisted electrodeposition. Li et al. [10] further revealed that rare-earth elements can be incorporated into the porous films for enhanced optical properties.

In comparison, reports that address the preparation of bulk ZnO foams are relatively limited, despite the clear importance of using the ZnO foams in chemical separations [7]. Lu and Xue [12] were the first to synthesize macroporous ZnO foams with an average pore size around 100–200 nm through a solvothermal process. Zinc peroxide (ZnO_2) was used as a precursor, which reduced chemically to form ZnO foams in organic solvent mixtures. They asserted that the release of O_2

*Corresponding author. Tel.: +886 422 870 720; fax: +886 422 857 017.
E-mail address: wenjea@dragon.nchu.edu.tw (W.J. Tseng).

0272-8842/$ - see front matter © 2013 Elsevier Ltd and Techna Group S.r.l. All rights reserved.
http://dx.doi.org/10.1016/j.ceramint.2013.09.005

bubbles as a by-product of the reduction reaction would accompany the ZnO formation so that a macroporous architecture was produced. In addition, a combustion process involving use of sodium chloride as both diluent and pore former was recently reported by Perraud et al. [7]. The macroporous ZnO foams prepared were used as an effective, regenerative adsorbent for the removal of sulfur in industrial chemical processes.

While the monolithic ZnO foams are useful in applications of chemical separation and purification, "additional" functions such as water disinfection, microbial control, and photocatalytic degradation of organic residues in wastewater and industrial effluent may be enhanced if silver (Ag) can be hybridized into the porous ZnO matrix [13–15]. A proper mineralization of the Ag particles with the ZnO foams is considered beneficial in minimizing the loss of Ag particles in service and avoiding difficulty in separation and re-use of the bactericidal particles from a suspension in comparison to the powdered counterpart, reducing hence potential biological and environmental concerns [14,15]. In this regard, we attempt to prepare macroporous ZnO foams through a solution route involving a preferential anchoring of hydrophobic ZnO nanoparticles at the air/water interface in order to stabilize the air-in-water droplets produced by a simple mechanical frothing. The wet foaming process is generally known as the Pickering emulsion [16,17] even though air-water system was used here instead of the frequently encountered water-oil system. The well-anchored ZnO particles at the interface provides an elastic and mechanically robust "shell" vital to prohibit coalescence, drainage (i.e., creaming), and disproportionation (i.e., Ostwald ripening) between neighboring bubbles over a given period of time typically in days or even weeks. A suitable wettability is hence critically important for the particles to reside successfully at the interface for rendering the foam stability [18,19]. In view of the literature, Gauckler and co-workers have recently proposed use of short-chain surfactant molecules in water to impart the hydrophobicity of originally hydrophilic ceramic surface in order for the preparation of ultrastable oxide foams with a tailored pore structure [20–22]. In our earlier reports [23,24], anionic sodium dodecul sulfate (SDS) was found capable of modifying the hydrophobicity of cationic gibbsite platelets in water through electrostatic interactions for preparing stable air-in-water gibbsite foams. In this study, we also use the SDS molecules to modify the surface of ZnO nanoparticles in water and examine effect of solids concentration (ϕ) of aqueous ZnO suspensions to the pore structure of ZnO foams prepared by the wet foaming route. A "one-pot" chemical preparation of wet ZnO-Ag composite foams is then explored for the first time.

2. Experimental procedure

2.1. Materials

ZnO nanoparticles (Centron Biochemistry Technology Inc., Taiwan) with mostly a rod-shaped morphology (Fig. 1) were used as the starting material. De-ionized (D.I.) water with an electrical resistivity of 18.2 Ω cm was from Millipore Super-Q Plus (U.S.A.). Reagent-grade SDS ($NaC_{12}H_{25}SO_4$, 99%, Aldrich, U.S.A.), 1-dodecanol ($CH_3(CH_2)_{11}OH$, 98.6%, Tedia, U.S.A.), ammonia (NH_4OH, 28%, Aldrich, Germany), and hydrochloric acid (HCl, 37%, Aldrich, Germany) were used without further purification for the surface modification and dispersion of the ZnO particles in water.

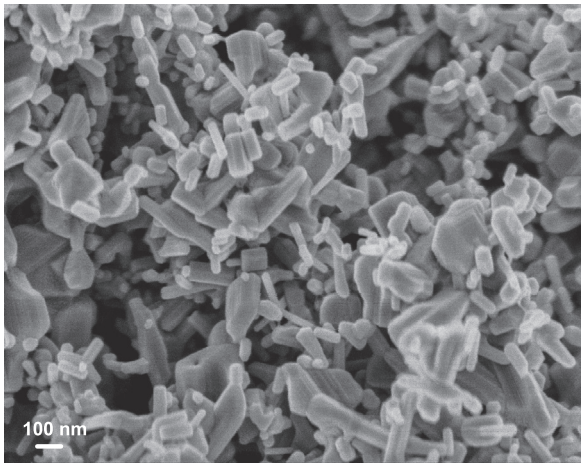

Fig. 1. Morphology of the as-received ZnO particles.

2.2. Surface modification and foam preparation

The as-received ZnO particles of 3.47 g were mixed with SDS, 0.03 g 1-dodecanol, and 20 ml D.I. water to form suspensions with ϕ of 3 vol%. The SDS concentration varied from 0–0.069 g, corresponding to a molar concentration range from 0–12 mM. pH of all the suspensions was adjusted to 6.1 by minor addition of HCl before being subjected to ball-mixing for 20 h. The surface-modified ZnO particles (i.e., those with the SDS addition) were filtered, oven-dried (65 °C for 24 h), and consolidated to form "green" ZnO discs ready for the contact-angle measurement.

The ZnO suspensions with various solids concentrations, i.e., ϕ ranges from 3–6 vol%, were also prepared. For the suspension with ϕ of 3 vol%, the SDS and 1-dodecanol concentrations were at 0.035 g (6 mM) and 0.03 g, respectively, in 20 ml of D.I. water. The weight of SDS and 1-dodecanol was increased in proportion as ϕ was increased above 3 vol%. Wet ZnO foams were all prepared by ball mixing, and the bubbles were collected and packed into non-porous molds followed then by oven drying at 65 °C for 24 h. The "green" foams were then sintered to 1400 °C with an isothermal holding of 1 h in ambient air.

To demonstrate the feasibility of extending the above particle-stabilized foaming process to the fabrication of wet composite foams, ZnO–Ag foam was prepared as a model material. Reagent-grade silver nitrate ($AgNO_3$, 99%, Aldrich, U.S.A.) of 1.7 g was dissolved in D.I. water (20 ml), before being added slowly in drops into an aqueous solution (20 ml) containing 25 vol% polyethylene glycol (PEG, molecular weight of 1000, Aldrich, U.S.A.) as a protective agent for avoiding the particle aggregation. The solution color changed from clear to black immediately after the addition of $AgNO_3$

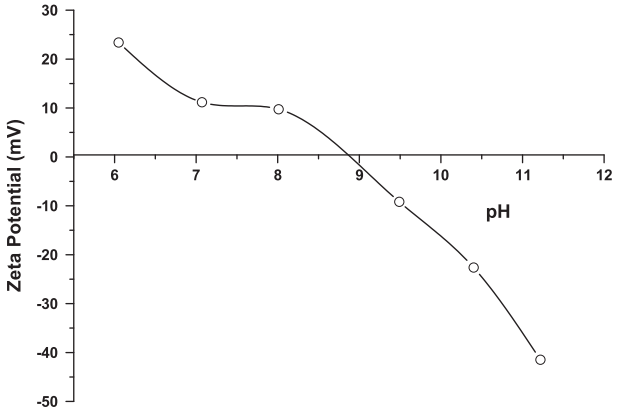

Fig. 2. Zeta potential of the as-received ZnO particles in water.

drops, indicating that the reduction of Ag took place in the solution. A ZnO suspension ($\phi = 6$ vol%) of 20 ml was prepared separately, and was then mixed with the reduced Ag colloid. The solution pH was adjusted to 6.1 before being mechanically ball-mixed for 20 h. Wet foams were then collected after the mixing operation, and shaped into bulk foams followed then by oven-drying. The dried ZnO–Ag foams were calcined to 600 °C with an isothermal holding of 1 h in ambient air.

2.3. Characterizations

Zeta potential of the ZnO particles was determined by the Zetasizer (Zetasizer NS, Malvern, U.K.) in water over a pH range from 6 to 11 using the laser Doppler electrophoresis. The suspensions were kept at a dilute concentration (~0.05 wt%) for the measurement, while the suspension pH was adjusted with HCl (2 M) and NH_4OH (1 M). Field-emission scanning electron microscopy (FE-SEM, JSM-6700 F, JEOL, Japan) equipped with energy-dispersive spectroscopy (EDS, Oxford Inca Energy 400, UK) was used for microstructural examination of the calcined ZnO and ZnO–Ag foams. A sessile drop-shape analyzer (FTA 2000, First Ten Angstroms Inc., U.S.A.) was used for the determination of *apparent* contact angle (θ); in which, water drops were dispensed from a syringe pointed vertically down onto the surface-smooth discs at 25 °C and water profiles on the samples were captured by an optical system. Details about the measurement can be found elsewhere [23,24]. At least five measurements were carried out for each batch of the foams prepared. In addition, mercury porosimetry (Autopore 9520, Micromeritics, U.S.A.) was used to measure the apparent pore size, pore volume, and bulk density (measured at pressure of 3.1 kPa) of the sintered foams. A maximum pressure of 414 MPa was used.

3. Results and discussion

3.1. Wettability of the SDS-modified ZnO surface

Fig. 2 shows zeta potential of the as-received ZnO particles in water. The isoelectric point (IEP) appears to fall at pH ~ 8.8, at which pH value the particles in suspension are expected to agglomerate spontaneously when approaching one another due to the lack of electrostatic repulsion to overcome the inter-particle attraction. At pH values lower than the IEP, the ZnO particles bear a net positive charge on the surface that is capable of attracting the polar end of anionic SDS molecules in water. In this regard, the particle charge at pH ~ 6 is considered beneficial in rendering the electrostatic stabilization of the ZnO suspensions (Fig. 2). Wet ZnO foams were hence prepared from the ZnO suspensions with $\phi = 3$ vol% at pH ~ 6 by varying the SDS concentrations from 0–12 mM. As shown in Fig. 3, preferential adsorption of the SDS molecules on the ZnO surface results in a pronounced increase of θ. An initially hydrophilic ZnO surface with $\theta \sim 32^\circ$ was changed to hydrophobic with θ approaches toward 90° through the electrostatic adsorption of polar head group of the anionic SDS molecules on the particle surface. The non-polar tail of the SDS molecules stretches toward the water medium, replacing then the initially hydrophilic ZnO surface so that the surface became more hydrophobic. In Fig. 3, the ZnO surface becomes apparently more hydrophobic when coverage of the SDS molecules was more complete on the particle surface when the SDS concentration

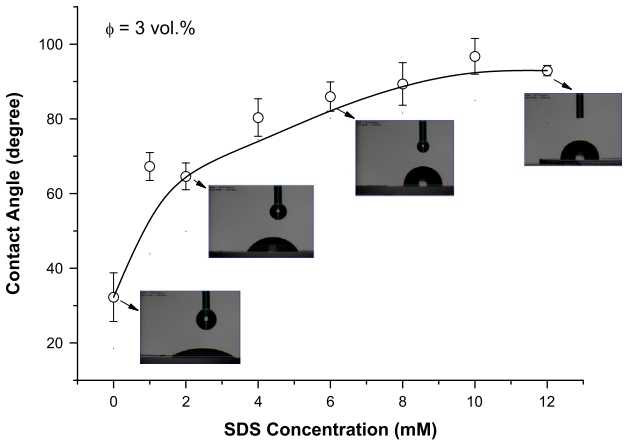

Fig. 3. SDS concentration to the contact angle of water on the ZnO particles. The solids concentration in the suspension state was at 3 vol%.

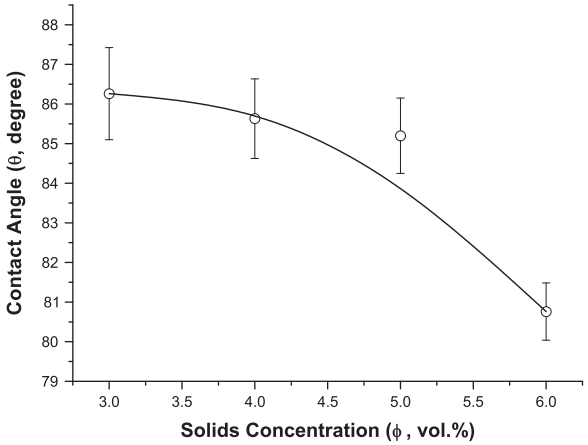

Fig. 4. Solids concentration of the ZnO suspensions to contact angle of water on the ZnO particles. The SDS concentration was held at 6 mM.

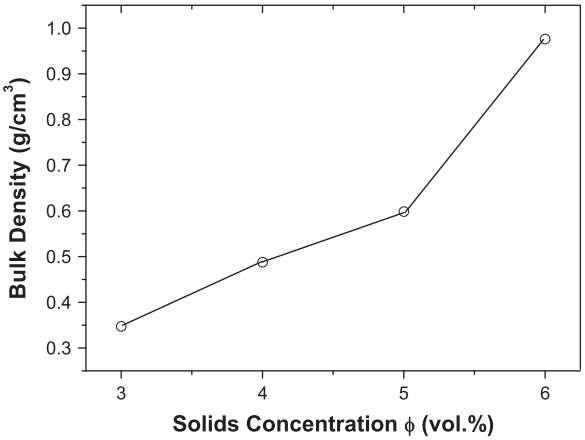

Fig. 5. Bulk densities of the ZnO foams fired at 1400 °C in ambient air. The densities were measured by mercury porosimetry at pressure of 3.1 kPa.

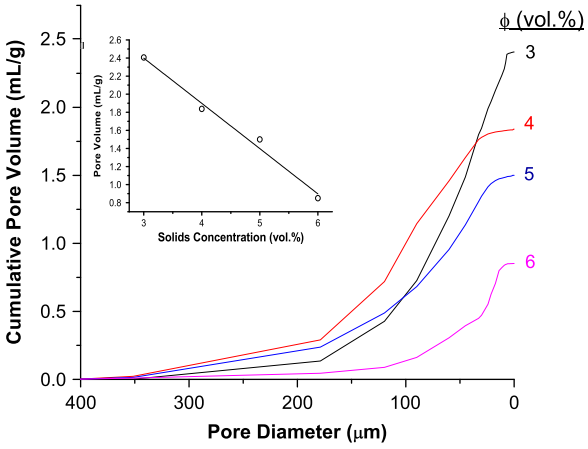

Fig. 6. Cumulative pore volume and Pore-size distribution of ZnO foams prepared from various solids concentrations in the suspension state. All the samples were calcined at 1400 C in air with 1 h dwell time.

increases. It may be interesting to note that the adsorption appears to follow a typical Langmuir adsorption; in which, the adsorption gradually reaches a saturation plateau when approaches the monolayer coverage. Therefore, the contact angle is seen to increase rapidly at first, follow then by a linear dependence with a reduced slope, and gradually reach a plateau as the SDS concentration was raised above ~8 mM. In Fig. 4 θ appears to reduce only slightly as ϕ was increased from 3 vol% to 6 vol%. It is worthy to note that the contact angle is still highly hydrophobic ($\theta > 80^{\circ}$) when the SDS concentration was held at 6 mM. This reveals that the adsorption of SDS molecules on the ZnO surface is not influenced much by the solids fraction used in the suspension; therefore, almost the same level of hydrophobicity is rendered by the SDS adsorption, so long as the monolayer coverage is attained.

3.2. Pore structure of the ZnO foams

Fig. 5 shows bulk density of the calcined ZnO foams. The bulk density increases from 0.35 to 0.95 g/cm^3 as ϕ was increased from 3 vol% to 6 vol%. All the ZnO foams prepared are porous with porosity ranging from 82% to 94% of the solids. This highly porous structure results because of the relatively low solids concentration used in the suspensions. Cumulative pore volume and pore-size distribution of the ZnO foams are shown in Fig. 6. A broad pore-size distribution ranging from ~20 to 160 μm is found; in addition, the pore volume appears to decrease linearly with ϕ. When ϕ was increased from 3 vol% to 6 vol%, the pore volume decreases pronouncedly from 2.41 mL g^{-1} to 0.85 mL g^{-1}, in good agreement with the bulk density observed. This pore-volume difference stemmed primarily from the degree of coverage of the nanoparticles anchored on the bubble surface in the wet foams. As shown in Fig. 7a, the foam prepared from the suspension of $\phi = 3$ vol% shows interconnected spherical

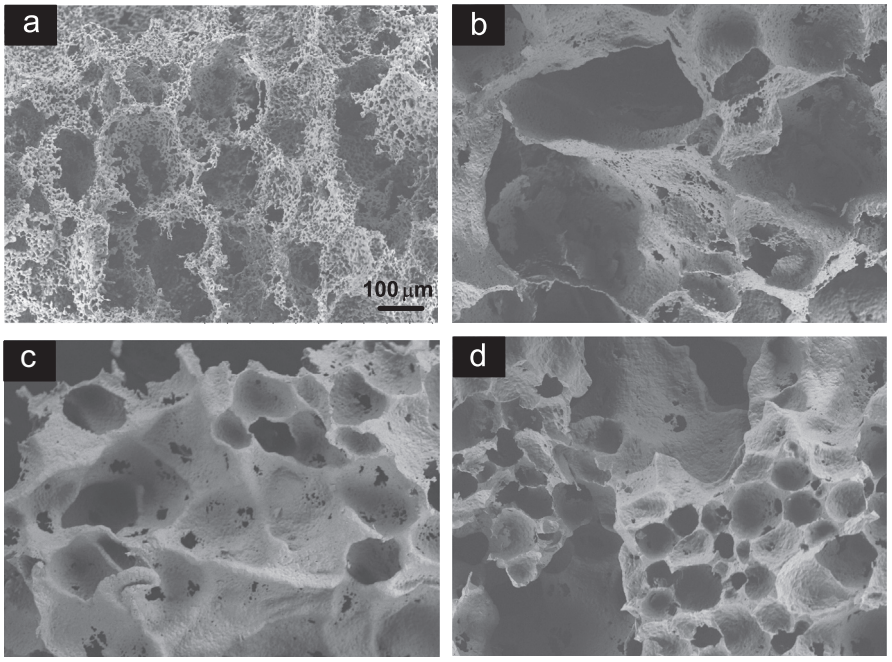

Fig. 7. Microstructure of the ZnO foams fired at 1400 °C in ambient air. The solids concentration used in the suspension state is (a) 3, (b) 4, (c) 5, and (d) 6 vol%, respectively.

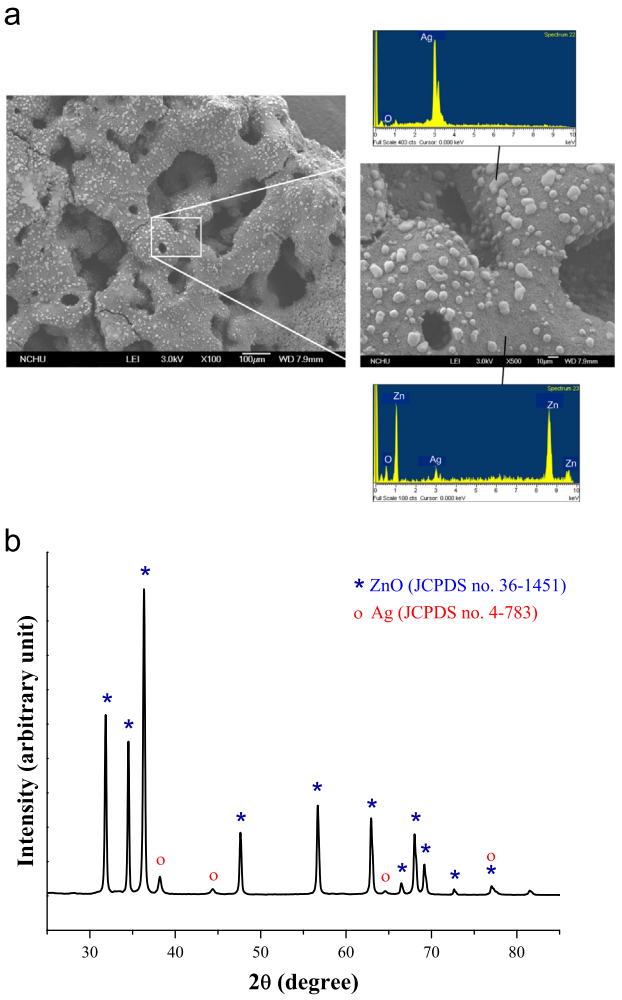

Fig. 8. (a) Microstructure and (b) XRD pattern of the ZnO–Ag composite foams fired at 600 °C in ambient air.

pores with a highly porous wall structure. This porous wall architecture results from an insufficient coverage of the ZnO particles on the foaming droplets. As ϕ increases to 4 vol%, the wall structure becomes apparently less porous in most regions (Fig. 7b), even though loosely packed porous walls are still found at some places. Further increase of ϕ (Fig. 7c and d) appears to result in a denser wall structure with a reduced occurrence of the loosely packed walls. This hence indicates that the number of hydrophobic ZnO particles available in the suspension to "protect" the air-in-water bubbles is critically important to the pore structure. An increasing ϕ would be beneficial to produce a denser wall structure at the expense of the maximum total pore volume attainable in the foams.

The foaming process is readily applicable to the wet preparation of composite foams. In Fig. 8a, porous ZnO foams decorated with a discrete distribution of Ag particles were prepared by the "one-pot" chemical route. The presence of ZnO and Ag in the calcined foams was confirmed by XRD in Fig. 8b; from which, mixture of crystalline phases is apparent. The EDS analyses show that the ZnO ceramics constitute the strut in the macroporous foam structure while the discrete Ag particles of micrometer size were "locked" on the ZnO surface. The process is facile, scale-up ready, and applicable to the fabrication of composite foams of different material combinations. More attempts are now underway in our laboratories.

4. Conclusions

Solids concentration has a pronounced influence on the pore structure of ZnO foams prepared by the direct foaming route. An increased solids concentration from 3 vol% to 6 vol% results in a more uniform coverage of the hydrophobic ZnO particles at the air-in-water interface, so that the wall structure becomes denser with a reduced occurrence of loosely packed porous walls. The high porosity ($>83\%$ in volume fraction) found in the ZnO foams is directly resulted from the low concentration of suspensions used in the foaming process. An interconnected pore structure with a broad pore-size distribution ($\sim$20–160 μm) is generally produced. The process is facile, flexible in shaping, easily scalable, and applicable to the fabrication of composite foams of different material combinations. For the first time, we have prepared interconnected, porous ZnO foams decorated with a discrete distribution of Ag particles on the ZnO struts.

Acknowledgments

We gratefully acknowledge financial support from the National Science Council (Taiwan) under contract numbers NSC 101-2221-E-005025-MY3, 101-2815-C-005-023-E, and 100-2815-C-005-016-E.

References

[1] K.C. Barick, S. Singh, M. Aslam, D. Bahadur, Porosity and photocatalytic studies of transition metal doped ZnO nanoclusters, Microporous and Mesopororous Materials 134 (2010) 195–202.
[2] C. Li, Z. Yu, S. Fang, H. Wang, Y. Gui, J. Xu, R. Chen, Journal of Alloys and Compounds 475 (2009) 718–722.
[3] J. Zheng, Z.-Y. Jiang, Q. Kuang, Z.-X. Xie, R.-B. Huang, L.-S. Zheng, Shape-controlled fabrication of porous ZnO architectures and their photocatalytic properties, Journal of Solid State Chemistry 182 (2009) 115–121.
[4] M. Muruganandham, I.S. Chen, J.J. Wu, Effect of temperature on the formation of macroporous ZnO bundles and its application in photocatalysis, Journal of Hazardous Materials 172 (2009) 700–706.
[5] H. Thakuria, B.M. Borah, G. Das, Macroporous metal oxides as an efficient heterogeneous catalyst for various organic transformations—a comparative study, Journal of Molecular Catalysis A Chemical 274 (2007) 1–10.
[6] M.A. McLachlan, H. Rahman, B. Illy, D.W. McComb, M.P. Ryan, Electrochemical deposition of ordered macroporous ZnO on transparent conducting electrodes, Materials Chemistry and Physics 129 (2011) 343–348.
[7] I. Perraud, R.M. Ayral, F. Rouessac, A. Ayral, Combustion synthesis of porous ZnO monoliths for sulfur removal, Chemical Engineering Journal 200–202 (2012) 1–9.
[8] B. Kılıç, E. Gür, S. Tüzemen, Nanoporous ZnO photoelectrode for dye-sensitized solar cell, Journal of Nanomaterials (2012) 474656.
[9] K.H. Yeo, L.K. The, C.C. Wong, Process and characterization of macroporous periodic nanostructured zinc oxide via electrodeposition, Journal of Crystal Growth 287 (2006) 180–184.

[10] G.-R. Li, C.-R. Dawa, X.-H. Lu, X.-L. Yu, Y.-X. Tong, Use of additives in the electrodeposition of nanostructured Eu^{3+}/ZnO films for photoluminescent devices, Langmuir 25 (2009) 2378–2384.
[11] E. Gür, B. Kılıç, C. Coşkun, S. Tüzemen, F. Bayrakçeken, Nanoporous structures on ZnO thin films, Superlattices and Microstructures 47 (2010) 182–186.
[12] P. Lu, D. Xue, Bubble-assisted nanofabrication of macroporous ZnO foams, Nanoscience and Nanotechnology Letters 3 (2011) 394–399.
[13] Q. Li, S. Mahendra, D.Y. Lyon, L. Brunet, M.V. Liga, D. Li, P.J.J. Alvarez, Antimicrobial nanomaterials for water disinfection and microbial control: potential applications and implications, Water Research 42 (2008) 4591–4602.
[14] W. Xie, Y. Li, W. Sun, J. Huang, H. Xie, X. Zhao, Surface modification of ZnO with Ag improves its photocatalytic efficiency and photostability, Journal of Photochemistry and Photobiology A: chemistry 216 (2010) 149–155.
[15] C. Marambio-Jones, E.M.V. Hoek, A review of the antibacterial effects of silver nanomaterials and potential implications for human health and the environment, Journal of Nanoparticle Research 12 (2010) 1531–1551.
[16] S.U. Pickering, Emulsions, Journal of the Chemical Society 91 (1907) 2001–2021.
[17] W. Ramsden, Separation of solids in the surface-layers of solutions and 'suspensions' (Observations on surface-membranes, bubbles, emulsions, and mechanical coagulation). Preliminary account, Proceedings of the Royal Society of London 72 (1903) 156–164.
[18] B.P. Binks, Macroporous silica from solid-stabilized emulsion templates, Advanced Materials 14 (2002) 1824–1827.
[19] O.D. Velev, K. Furusawa, K. Nagayama, Assembly of latex particles by using emulsion droplets as templates. 1. Microstructured hollow spheres, Langmuir 12 (1996) 2374–2384.
[20] U.T. Gonzenbach, A.R. Studart, E. Tervoort, L.J. Gauckler, Ultrastable particle-stabilized foams, Angewandte Chemie International Edition 45 (2006) 3526–3530.
[21] U.T. Gonzenbach, A.R. Studart, E. Tervoort, L.J. Gauckler, Macroporous ceramics from particle-stabilized wet foams, Journal of the American Ceramic Society 90 (2007) 16–22.
[22] I. Akartuna, A.R. Studart, E. Tervoort, L.J. Gauckler, Macroporous ceramics from particle-stabilized emulsions, Advanced Materials 20 (2008) 4714–4718.
[23] W.J. Tseng, P.-S. Wu, Effect of sodium dodecul sulfate on stability of gibbsite platelet stabilized emulsion foams, Ceramics International 38 (2012) 2711–2718.
[24] W.J. Tseng, P.-S. Wu, Macroporous gibbsite foams prepared from particle-stabilized emulsions using corn starch and agar as binders, Ceramics International 38 (2012) 4461–4465.